Journal of Theoretical and Applied Information Technology
15th November 2024. Vol.102. No. 21

ISSN: 1992-8645 www.jatit.org E-ISSN: 1817-3195

ADVANCED LIGHTWEIGHT ST-TCN FRAMEWORK USING UAV MULTI-SPECTRAL REMOTE SENSING FOR SURVEILLANCE AND CONTROL OF PINE NEMATODE DISEASE

Dr. J. DEEPA[1], Dr. V. GOKULA KRISHNAN[2,*], Dr. S. VENKATA LAKSHMI[3], Dr. D. ARUL KUMAR[4], Dr. V. VIJAYARAJA[5]

[1]Associate Professor, Department of CSE, Easwari Engineering College, Chennai, Tamil Nadu, India.
[2,*]Professor, Department of CSE, Saveetha School of Engineering, Saveetha Institute of Medical and Technical Sciences, Thandalam, Chennai, Tamil Nadu, India
[3]Professor & Head, Department of AI & DS, Sri Krishna College of Engineering and Technology, Coimbatore, Tamil Nadu, India
[4]Associate Professor, Department of ECE, Panimalar Engineering College, Poonamallee, Chennai, Tamil Nadu, India
[5]Associate Professor, Department of AI & DS, RMK College of Engineering and Technology, Kavaraipettai, Tamil Nadu, India

Email: [1]deepa.j@eec.srmrmp.edu.in, [2,*]gokul_kris143@yahoo.com, [3]venkatalakshmis@skcet.ac.in, [4]arul.annauniv@gmail.com, [5]vijayarajaads@rmkcet.ac.in

ABSTRACT

The pine nematode is a highly infectious disease that devastates pine forests globally, necessitating prompt and precise diagnostic approaches. However, existing methods face challenges in accurately identifying and localizing nematode infections within individual trees, with limited studies addressing these gaps. This research contributes a novel artificial intelligence-based approach that leverages multi-spectral remote sensing imagery captured by unmanned aerial vehicles (UAVs) to diagnose pine nematode infections. By utilizing lightweight special task temporal convolutional network (ST-TCN) blocks and multiple bottleneck layers, our model focuses on critical features in the input sequence. This enables the classifier to differentiate between various diseases effectively. We further improve classification accuracy by fine-tuning model parameters through a Cat Swarm Updated Black Widow (CSUBW) optimization algorithm. The proposed method offers a rapid, accurate, and practical solution for monitoring and managing pine wood nematode disease, marking a significant advancement in the detection and control of this infection.

Keywords: *Unmanned Aerial Vehicle, Special Task Temporal Convolutional Network, Cat Swarm Updated Black Widow Model, Remote Sensing Images, Pine Nematode Disease.*

1. INTRODUCTION

Pinewood nematode (Bursaphelenchus xylophilus) causes pine wilt disease (PWD), which disrupts water and nutrient flow in pine trees, leading to dehydration and death [1]. Two primary vectors, Monochamus alternatus and Monochamus saltuarius, spread this disease across regions in East Asia, including the Korean Peninsula, where different species inhabit distinct climatic zones. Southern regions, warmer parts of Japan, and southern China are home to M. alternatus, while M. saltuarius is prevalent in colder zones such as central Korea, northeast China, and parts of Russia and Finland [2, 3]. The infection particularly affects black pine, Japanese red pine, and Korean white pine in Korea [4]. Initially identified in North America, PWD has become the most destructive forest disease in East Asia, severely impacting forests in Japan, China, Korea, and extending into Europe, where it has damaged pine trees in Portugal. This disease not only degrades the environment but also disrupts local economies, emphasizing the need for robust forest health measures and quarantine practices in affected regions [5, 6].

Detecting and controlling PWD remains a challenging task due to its rapid spread and the high

cost of conventional ground-based monitoring methods. UAVs equipped with advanced imaging sensors offer an efficient alternative by enabling remote, cost-effective pest detection through multi-spectral imaging and object detection models [7]. However, traditional monitoring struggles to accurately track the spread of PWD, especially given the spread of pests to new areas as climate change allows subtropical pests to survive in temperate climates, while warming winters allow localized pests to thrive [8, 9]. Early detection, combined with tree removal and fumigation, is the most effective strategy to prevent PWD spread, but conventional land monitoring presents financial and logistical limitations [10]. Recent efforts have explored the potential of UAV footage in detecting PWD, focusing on time-series data, multispectral footage, and vegetation indices [11].

Due to the extensive data generated by UAV networks, managing large volumes of multi-spectral footage requires automated, computationally efficient methods. Manually created feature-based algorithms are insufficient in handling such complex datasets, highlighting the need for deep learning (DL) and deep neural network (DNN) methods that can autonomously learn critical features for PWD detection [12]. Convolutional DNNs, inspired by the structure of the animal visual cortex, have proven effective for image processing, but traditional approaches lack accuracy when applied to diseases requiring an analysis of temporal and spatial relationships in the data [13, 14].

The need for an accurate and computationally efficient approach to diagnosing PWD leads to the following research contributions:

- We introduce a bottleneck layer to improve the model's ability to analyze local motion between frames, capturing spatial and temporal correlations more effectively than traditional methods. This bottleneck layer, applied here for the first time to disease diagnosis, enhances detection accuracy and reduces latency in real-time applications.
- Our proposed model uniquely combines bottleneck layers with a temporal convolutional network (TCN) for feature extraction, allowing for a more precise distinction of disease symptoms. This network learns important signals from multi-spectral UAV images, surpassing traditional methods in terms of diagnostic performance.
- For further enhancement, we employ a Cat Swarm Updated Black Widow (CSUBW) optimization model to fine-tune parameters, thereby boosting classification accuracy through optimized feature selection.

In summary, this research aims to address the limitations of existing PWD detection methods by proposing a novel AI-based solution for prompt, accurate, and scalable monitoring of pine nematode infections, offering a significant advancement in forest health management.

The rest of the paper is organized as follows: Section 2 references the related works; Section 3 presents the projected methodology and its explanation; Section 4 demonstrates the results analysis and finally, the conclusion of the research work is given in Section 5.

2. RELATED WORKS

As a lightweight approach to pine wilt disease detection, Yuan et al. [16] provide Light-ViTeYOLO, which is based on Vision Transformer-enhanced YOLO. The EfficientViT feature extraction network is built using a new lightweight multi-scale attention module that allows for multi-scale learning. To improve localization accuracy, a new neck network called CACSNet (Content-Aware neck network) is optimized for loss function, and it is meant to better diseased tree detection at single granularity. The approach manages to improve detection performance while simultaneously decreasing the detection model's parameter count and GFLOPs. In comparison to existing baseline algorithms, the experimental results show that the proposed Light-ViTeYOLO algorithm in this study has the lowest parameter complexity (3.89 MFLOPs) and computational complexity (7.4 GFLOPs) among relevant algorithms. With 57.9 frames per second, it outshines the original YOLOv5. Aside from a small drop in recall and mAP@0.5, its mAP@0.5:0.95 ranks highest among baseline algorithms. Pine wilt disease detection has never been easier than with our Light-ViTeYOLO. Both the needs for automated forestry operations and the need for real-time detection of pine wilt disease outbreaks are met by it. How can lightweight deep learning models be enhanced to improve both detection accuracy and computational efficiency for identifying pine wilt disease (PWD) across

different tree species and disease stages in large forest areas?

In the Dahuofang Experimental, Liaoning Province, Xie et al., [17] used UAVs to take pictures of pine trees in the early stages of PWD infection. In order to help with future studies on detecting early-stage infestations in pine trees, a dataset of early infected trees afflicted by PWD has been compiled. On the early-stage PWD dataset, the top-performing approach outperforms Faster R-CNN, DETR, and YOLOv5 with improvements of 17.7%, 6.2%, and 6.0% in average precision (AP) and 14.6%, 3.9%, and 5.0% in F1 scores, respectively. What techniques can be developed to generate realistic synthetic data that closely approximates the characteristics of PWD in natural forest settings, thereby improving model generalizability? As a first step towards early treatment of pine wood nematode disease, the study offers technological support for field-based early-stage PWD tree counting and localization in forested areas.

Using YOLOv8 to segment sick areas, cropping the diseased portions from the original image, and applying Deep Metric Learning for classification, Thapa et al., [18] proposes a novel classification. After extracting embedding's from a ResNet50 model trained with semi-hard triplet loss, we trained a Random Forest classifier to distinguish between false positives and identify tree species. We chose segmentation over object detection because it can provide us information down to the pixel level, which allows us to easily extend the bounding boxes that come after it. The efficiency of Deep Metric Learning in processing visually comparable images led to its selection as the classification method following segmentation. The segmentation findings show an average Union of 83.12%, with test set classification accuracies of 90.7% and validation set accuracies of 98.7%.

We constructed our synthetic dataset based on the virtual forest that Jung et al. [19] describes, which takes people with disabilities into account and was rendered using 3D techniques. Our use of Image-to-Image (I2I) translation methods further guarantees that the simulated data will closely match the original. For this purpose, we compared the output of each dataset using the EfficientNetv2-S model. We validated that our model, which was trained exclusively on the PWD synthetic dataset, had the capability to recognize actual PWD. With an F1 Score of 92.88%, the model that was trained using an ensemble that included both real and synthetic data performed even better. Improved presentation was also seen when an ensemble of actual and synthetic data was translated using the I2I technique. This finding lends credence to the study's proposed synthetic data and demonstrates its usefulness. What advanced optimization methods can be applied to fine-tune model parameters for enhanced classification and localization of PWD, enabling rapid and scalable disease detection in real-world environments? It is believed that this study's results will have implications for agricultural management and the wider preservation of forest ecosystems through their applicability to the identification of diseases in different types of forests.

The monthly outbreak timing and dissemination distances of PWD have been studied by Tan et al., [20]. The study focused on two areas in southeastern China, A and B, which were identified by different proportions of broadleaf and coniferous trees. There were four distinct phases of infection inflicted on trees: early, medium, late, and dead. To determine the stress stages and tree locations, three deep learning procedures—namely, Faster R-CNN, YOLOv5, and YOLOv8—were used in conjunction with monthly RGB data collected by an unmanned aerial vehicle (UAV) over the course of a year. In addition, the distances from the site of neighboring trees were calculated by recording the number of newly afflicted trees each month. The YOLOv5 model outperformed the others with the best accuracy (mAP = 0.58, F1 = 0.63) in the study. Faster R-CNN came in second with mAP = 0.55, F1 = 0.58, and YOLOv8 came in third with mAP = 0.57, F1 = 0.61). In the months of August and September, there were early and middle-stage PWD outbreaks, and in the months of October and February of the following year, there were late-stage and dead-tree outbreaks. During the course of a year, the average nearest spread distance for PWD-infected trees in regions A and B was 12.54 m (median: 9.24 m) and 13.14 m (median: 10.26 m), respectively. According to the results, the best time to control PWD is between the months of February and August. Also, forests that are mixed conifer and broadleaf, with a higher percentage of broadleaf trees, help reduce the severity of PWD outbreaks. How can the integration of outbreak timing and spread distance data with UAV-based detection models provide actionable insights for controlling PWD spread and improving disease management strategies?. This study provides technical help for the control and

management of forest pests by demonstrating the efficacy of using deep learning algorithms in conjunction with monthly UAV-based imagery to track the timings and distances of PWD outbreaks.

Problem Statement:

1. Existing methods for detecting pine wilt disease (PWD) struggle with accurately identifying and localizing infections across different tree species and disease stages in real-world forest environments.
2. Although lightweight models (e.g., Light-ViTeYOLO) improve detection speed, they face limitations in recall and precision, particularly in detecting early and subtle signs of infection.
3. Synthetic data approaches help augment training data, yet there remains a gap in generating simulated data that closely mirrors real-world PWD characteristics, impacting model generalizability.
4. Current studies on PWD spread timing and distances indicate a need for methods that integrate multi-spectral data to track disease progression at the individual tree level.
5. A scalable, high-accuracy solution is needed that combines multi-spectral UAV imagery with advanced deep learning techniques for efficient, large-scale PWD monitoring and early intervention.

3. PROPOSED MODEL

The disease detection is carried out by UAV images from drones and uses the ST-TCN network, which is shown in Figure 1.

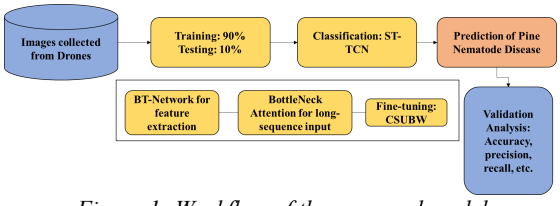

Figure 1: Workflow of the proposed model

3.1. Data Information

The FeimaD200 quadrotor served as the experimental platform for aerial flying. The UAV was outfitted with a multi-spectral camera, namely a RedEdge-MX model, which possesses green (475 nm), red bands [21]. We were able to get four photographs using the UAV [22]. You may find all the relevant data in Table 1. These regions can be found throughout central and eastern China. In Anhui, you may find Huangshan-1 and Huangshan-2. A small number of hardwood trees complement the more common bamboo and Masson pine. In the flight area, you can see mixed woodlands near Wuhan, which is in Hubei. Shandong is home to Yantai and is mostly forested with coniferous trees. The training data set included Huangshan-2, whereas the test sets included Huangshan-1, Wuhan, and Yantai.

Table 1: Flight Limits

Images	Huangshan-1	Huangshan-2	Wuhan	Yantai
Discover	Anhui Area	Anhui Area	Hubei Area	Shandong Area
Flight height	170 m	170 m	200 m	160 m
Spatial resolution	0.1 m	0.1 m	0.175 m	0.1 m
Flight date	2019-08-12	2019-08-13	2019-8-21	2019-10-16
Wavelength (nm)	Blue: 475 nm RedEdge: 740 nm Green: 560 nm Red: 670 nm Near IR: 840 nm			

A data acquisition technique without picture control was used for this experiment since the UAV flight platform used had a real-time kinematic scheme, which meant that high-precision foreign copy elements were delivered. When creating multi-spectral orthographic photos, several steps were involved, such as orienting the camera internally, choosing a coordinate system, calibrating the radiation, registering the bands, using aerial triangulation, creating a digital elevation model, and finally, creating the photographs themselves. Figure 2 shows the results of the radiometric calibration that was conducted prior to flight using a diffuse plate [23].

Figure 2. UAV besides diffuse plate.

3.2. Dataset Details

This work uses the Huangshan-2 image as a data sample, and then uses a visual interpretation approach to create vector data of pine nematode illness and produce the associated label. To avoid over fitting models and increase sample size and diversity, multi-scale segmentation is useful. Hence, the label data and Huangshan-2 photos were split into 128 × 128 pixels and 256 × 256 pixels, respectively. After merging, a base for the pine nematode disease identification prototypical was created. The data sample was erratically split into a training set and a ratio of 3:1 in order to evaluate the model's validity. There were 4862 sub-images in the training data after a small number of invalid samples were removed, and 1712 sub-images were confirmed. In Figure 3, a few examples are given.

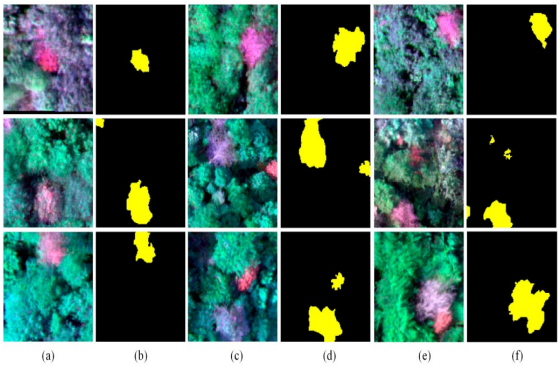

Figure 3. Sample Dataset (a, c, e: Imageries) (b, d, f: Labels)

3.3. Spatial Task Temporal Convolution Network (ST-TCN)

The study proposes the ST-TCN blocks as a feature extractor as an alternative of traditional RNNs, which use feedback loops to propagate information through time. But our TCN uses temporal convolutions to capture long-term dependencies in the input sequence. The input sequence is fed into a stack of convolution layers. In contrast, each layer applies a filter to a sequence of input values, with the other attributes determining the size of the receptive field. Therefore, by stacking multiple convolution layers with increased receptive field, TCN can capture dependencies over increasingly long periods. We designed three blocks of the ST-TCN in a hierarchical manner to learn features efficiently and make them parallelized for long sequence processing. Each block is connected hierarchically with input to capture deeper and hidden features from long sequences.

Each ST-TCN block consists of Input, a sequence of data points, and a tensor of shape (sequence length, input dimension), convolutional layers. The convolution filters have a fixed size and are convolved over the input sequence with a specified receptive field. After each layer, an activation function is applied to the layer's output with residual connections to improve the flow of gradient in training and alleviate the vanishing gradient problem. Our network often includes residual connections that bypass some of the convolutional layers. This allows the network to learn the input sequence's short- and long-term dependencies. Similarly, down sampling and up sampling are used to lessen the dimensionality of the output besides extract the key features from the sequence. Through this, we capture long-term dependencies in the input sequence using a stack of layers, enhancing the system efficiency and scalability for real-time.

3.3.1. Bottleneck Transformer Network (BTNet)

In [24], an updated version of the conventional transformer design was presented: the bottleneck transformer. For long input sequences, the computing cost of applying the self-attention mechanism to each token can be prohibitive. A visual representation of the BTNet's updated workflow. Before being combined with the remaining tokens and transferred to the next layer, a

subset of the input tokens is randomly chosen and processed by a reduced number of attention layers in a bottleneck transformer. As a result, the architecture becomes more computationally efficient by reducing the number of attention layers required. Following this same approach, we trained the classic bottleneck transformer network (BTNet) in a manner analogous to that of regular transformers, using back propagation and gradient descent optimisation, and then optimized it for detection tasks. We used the dimensions of the imputed tensor to capture the content's position, and then we parallel connected it to the original material in order to highlight important signals. With fewer computational resources needed, the suggested BTNet outperformed the standard.

There are two sections to the suggested BTNet's learning technique when dealing with the input sequence: the "core" sequence and the "context" sequence. Many attention layers work independently to process the context sequence. The forward layer receives a combined set of core and context sequences. Merging the two sequences and applying a linear projection layer is all that's needed to achieve the combo. This can be done on different levels at the same time. While lowering the number of attention layers given to the main sequence. The suggested BTNet is able to attain better computational efficiency without sacrificing performance because of this approach. To further regularize the network and avoid over fitting, we used various pattern dropout techniques. Instead of removing individual weights during training, complete attention weight patterns are randomly dropped. The approach enhances the network's capacity to generalize to new data and motivates it to learn stronger representations.

3.3.2. Bottleneck attention

The bottleneck attention mechanism [25] is a technique used in deep learning to improve the efficiency of attention-based models. Attention mechanisms are used to selectively focus on essential parts of input data when dealing with long sequences. Bottleneck attention reduces input dimensionality, cutting costs while preserving crucial information. Our proposed bottleneck includes a sequential and spatial layer, with an attention mechanism operating on the reduced-dimensional representation using standard do product attention. Our suggested module calculates the final feature map by:

$$F' = F + F * M(F) \quad (1)$$

$$M(F) = \alpha M_s(F) + M_c(F) \quad (2)$$

$$M_s = BN(FC(AP(F))) = BN(w_1(w_0 AP(F) + b_0) + b_1) \quad (3)$$

$$M_c(F) = Seq(\int_{l1}^{n}), (\int_{l2}^{n}), (\int_{ln}^{n}(F)) \quad (4)$$

$$F' = (1 + M(F))F(x, \theta) \quad (5)$$

$$\frac{\alpha M(F)F(x,\theta)}{\alpha\theta} = M(F)\frac{\alpha F(x,\theta)}{\alpha\theta} \quad (6)$$

There are three components to the attention weights: Ms(F) for spatial features, Mc(F) for temporal cues, and M(F) for the final weights. The preceding method shows that gradients and attentions value are directly related. The inverse is also true: larger attention values necessitate larger gradient values. The constraints used in feature extraction are represented by the symbol θ. Consequently, humans pay close attention to important signals by employing attention processes like channel-wise. Spatial attention eliminates noise and targets crucial spatial locations via dense layers rather than selecting an object region apart from channel focus. Combining these two attentional systems is crucial for activities because they employ complimentary information.

We were able to zero in on the exact objectives of each branch in the input tensor thanks to our attention map implementation, which led to a very effective strategy. A linear projection or other dimensionality reduction layer is one component of our attention module that takes an input sequence. Often referred to as the "bottleneck layer," this layer limits the amount of data that can reach the attention mechanism. An attention mechanism takes a lower-dimensional representation of the input sequence and uses it to determine the relative relevance of each element by giving it a weight. You can provide more weight to significant parts and less weight to irrelevant ones by using the weighted sequence and the attention weights that come from it to weight the input sequence. The result is a prioritized list with the most important details highlighted. All of the model's components get their input sequence attention weights from this process.

3.3.3. Fine-tuning of the model using CSUBW

The CSO was designed with insights gained from studying feline behaviour. Because of its improved convergence, the CSO model is able to resolve complex optimisation problems. Both "seeking mode" and "tracking mode" describe the typical behaviors of cats. Also, black widow spiders' "unique mating behaviour" served as inspiration for the BWO. Strongly convergent solutions to complicated optimisation issues are likewise efficiently handled by the BWO model. In addition, the search agents find global keys in the search space in this scenario. The literature states that conventional algorithms need lower levels of convergence than hybrid optimisation models. In this work, we combined the BWO [26] with the CSA model; thus, the suggested hybrid approach is the CSUBW model. What follows is a breakdown of the CSUBW model's steps

Step 1: Put the search agent's M population (pop) into its initial state in the space with dimensions D. The search agent's position is indicated by X, and its velocity is marked.

Step 2: The cats are dispersed at random across the three-dimensional space, and the value is chosen at random from the range of possible velocities.

Step 3: The tracing mode is activated after the "mixture ratio (MR)" and the number of cats have been determined. All of the surviving cats are now on a never-ending hunt.

Step 4: Looking for Manner

1. Seeking Mode: for the present cat Cat_k, J made. Here, J is the SMP. If SPC charge = true, then set J = (SMP-1) and set the existing cat as the best one.
2. As per CDC, the SRD values are indiscriminately minus. Then, substitute the old ones with the current ones.
3. For entirely the candidate topics, the fitness is calculated using Equation (7).

$$Pos_i = \frac{Fit_i - Fit_b}{Fit_{max} - Fit_{min}}, where 0 < i < j \quad (7)$$

4. For each candidate point, the selection probability is calculated when they are not equal. When all of the candidate points have an equal fit, the choosing probability is set to 1.
5. Here, minimizing is the goal, therefore, $Fit_b = Fit_{max}$
6. The point is selected at random to depart from the candidate points, and the cats' positions are swapped out.

Step 5: Proposed Tracing Style: When mode, the cat's speed is independent in all directions. What follows is an illustration of the procedures used in the tracing model:

(a) Equation (8) provides a newly proposed expression that is used to update the search agent's velocity for every dimension.

$$V_{j_{new}}^{d+1} = \omega V_j^d + \beta\left(P_g - X_j^d\right) + \alpha \times \epsilon \quad (8)$$

In this case, w is the mass of inertia besides e is the velocity of random variables distributed uniformly over the intermission [0, 1]. Furthermore, α and β are the parameters that regulate the process. According to Equations (9) and (10), the mathematical parameters a(t) and b(t) can be utilized to regulate the cats during the exploring phase, respectively. The variables a(min) and a(max) indicate the lower and upper bounds, respectively. A current iteration is pointed as t, and the maximal iteration is denoted as t(max). Additionally, b(min) represents the value of the initial iteration and b(max) represents the value of the final repetition.

$$\alpha(t) = \alpha_{max} - \frac{\alpha_{max} - \alpha_{min}}{t_{max}} \times t \quad (9)$$

$$\beta(t) = \beta_{min} + (\beta_{max} - \beta_{min}).Sin\frac{\pi t}{t_{max}} \quad (10)$$

(b) Before proceeding, be sure the speed is not higher than the maximum speed. If the new speed is beyond the allowed maximum speed range, then set limit.

(c) Update the site of Cat_k going with the BWO's update model instead of the old-fashioned CSA update function. The Mutepop number is chosen at random from the population (pop) via the mutation update model. The Mutepop is calculated using the mutation rate.

Step 6: Find the search agent's fitness using Equation (7). We say that the optimal choice is the cat whose fitness function is the highest. X_{best}.

Step 7: The cats are enthused grounded on their flags; if the cat Cat_k is determined to be in seeking mode, then processes in seeking mode; otherwise, processes in tracing mode.

Step 8: Determine the number of cats once more using the MR, and then put them into either searching or tracing mode.

Step 9: Terminate.

4. RESULTS AND DISCUSSION

The trials are conducted on a PC with an Intel Core i5-7200 CPU, 8 GB of RAM, and a processing speed of 2.7 GHz. A specialized user interface (UI) and Jupiter Notebook (Python 3.7) are utilized to execute the procedures on Windows 10, a 64-bit operating system. Natural Setting.

4.1. Validation Analysis of Proposed Classifier

Table 2 and Figure 4 deliver the comparative investigation of proposed classifier with existing techniques in terms of unlike metrics.

Table 2: Validation analysis of proposed model

Metrics	AlexNet	VGG19	SqueezeNet	Proposed
Accuracy	0.9588	0.9671	0.9788	0.9971
Precision	0.9417	0.9510	0.9645	0.9801
Sensitivity	0.9524	0.9645	0.9797	0.9877
Specificity	0.9614	0.9788	0.9866	0.9973
F1-Score	0.9553	0.9410	0.9446	0.9625
Time [minutes]	21.31	19.76	17.19	15.48

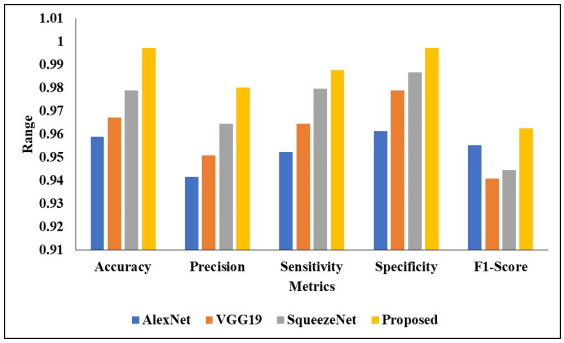

Figure 4: Graphical Comparison of proposed model

In above table 2 and figure 4 represent the Validation study of projected model. In the analysis of Accuracy calculation of AlexNet technique as 0.9588 also VGG19 technique of 0.9671 and squeeze technique as 0.9788 and also proposed technique as 0.9971 correspondingly. Then the Precision calculation of AlexNet technique as 0.9417 also VGG19 technique of 0.9510 and squeeze technique as 0.9645 and also proposed technique as 0.9801 correspondingly. Then the Sensitivity calculation of AlexNet technique as 0.9524 also VGG19 technique of 0.9645 and squeeze technique as 0.9797 and also proposed technique as 0.9877 correspondingly. Then the Specificity calculation of AlexNet technique as 0.9614 also VGG19 technique of 0.9788 and squeeze technique as 0.9866 and also proposed technique as 0.9973 correspondingly. Then the F1-Score calculation of AlexNet technique as 0.9553 also VGG19 technique of 0.9410 and squeeze technique as 0.9446 and also proposed technique as 0.9625 correspondingly. Then the Time [minutes] calculation of AlexNet technique as 21.31 also VGG19 technique of 19.76 and squeeze technique as 17.19 and also proposed technique as 15.48 correspondingly.

4.2. Validation Study of Proposed Optimization

Table 3 delivers the experimental study of proposed optimization with existing models in terms of unalike metrics.

Table 3: Comparative analysis of proposed optimization.

Metrics	ABOA	CSOA	BWOA	CSUBW
Accuracy	0.9388	0.9571	0.9688	0.9701
Precision	0.9147	0.9251	0.9405	0.9617
Sensitivity	0.9324	0.9415	0.9597	0.9770
Specificity	0.9514	0.9688	0.9766	0.9873
F1-Score	0.9153	0.9241	0.9346	0.9550

In Table 3: Comparative analysis of proposed optimization.in the analysis of Accuracy estimations of ABOA technique attained as 0.9388 also CSOA technique as 0.9571 and BWOA technique as 0.9688 and also CSUBW technique rate as 0.9701 correspondingly. Then the Precision estimations of ABOA technique attained as 0.9147 also CSOA technique as 0.9251 and BWOA

technique as 0.9405 and also CSUBW technique rate as 0.9617 correspondingly. Then the Sensitivity estimations of ABOA technique attained as 0.9324 also CSOA technique as 0.9415 and BWOA technique as 0.9597 and also CSUBW technique rate as 0.9770 correspondingly. Then the Specificity estimations of ABOA technique attained as 0.9514 also CSOA technique as 0.9688 and BWOA technique as 0.9766 and also CSUBW technique rate as 0.9873 correspondingly. Then the F1-Score estimations of ABOA technique attained as 0.9153 also CSOA technique as 0.9241 and BWOA technique as 0.9346 and also CSUBW technique rate as 0.9550 correspondingly.

4.3 Limitations and Issues

A key limitation is the dependency on high-quality UAV-based multi-spectral imagery data, which may not be available for all forested regions. Disease progression is influenced by environmental factors (e.g., climate, soil quality, and forest composition) and seasonal changes, which may impact the model's generalizability across different regions and times of the year. Balancing the need for high accuracy with the limitations of computational resources remains challenging. While the model can identify infection in real-time, there remains an open issue regarding the integration of long-term monitoring data to predict disease spread and assist with proactive interventions. Adapting the model to environmental variability across diverse ecosystems is an on-going challenge. While this study focuses on PWD, the adaptability of the model for detecting other forest diseases remains unexplored.

5. CONCLUSION

This study introduces a novel framework for detecting pine wood nematode disease (PWD) through UAV-captured multi-spectral imagery, addressing key challenges in achieving high accuracy, scalability, and efficiency in forest disease monitoring. Our approach incorporates a spatial information retention module to capture essential low-level features, an attention refinement module to accentuate disease-specific indicators, and a context information module to broaden the model's receptive field. Together, these components tackle the critical need for precise PWD identification, as outlined in our problem statement, by effectively isolating disease-related characteristics from background noise. The experimental results confirm the proposed model's accuracy and robustness in identifying PWD across different stages, directly supporting our objective of enhancing detection accuracy across species and progression levels. Unlike traditional methods, which often suffer from feature loss and require significant computational resources, our framework successfully retains critical spatial information and selectively highlights disease traits, leading to marked improvements in detection precision and processing efficiency. The model also demonstrated superiority over current state-of-the-art techniques, aligning with our objective of creating a high-performance solution suitable for real-time forest health management. With scalability in mind, the model holds promise for broad application across different forest disease scenarios, thus fulfilling the need for sustainable and proactive forestry solutions. Future work will focus on testing the model with additional datasets that cover diverse environmental conditions and a range of disease types. This testing will help evaluate the model's adaptability, address potential limitations, and refine it for broader applicability. Overall, this research contributes a powerful tool for effective PWD detection and offers significant potential for safeguarding forest ecosystems against disease threats through timely and precise interventions.

REFERENCES:

[1] Zhang, Z., Wang, B., Chen, W., Wu, Y., Qin, J., Chen, P., ... & He, A. (2023). Recognition of abnormal individuals based on lightweight deep learning using aerial images in complex forest landscapes: a case study of pine wood nematode. Remote Sensing, 15(5), 1181.

[2] Li, H., Chen, L., Yao, Z., Li, N., Long, L., & Zhang, X. (2023). Intelligent identification of pine wilt disease infected individual trees using UAV-based hyperspectral imagery. Remote Sensing, 15(13), 3295.

[3] Jung, Y., Byun, S., Kim, B., Amin, S. U., & Seo, S. (2024). Harnessing synthetic data for enhanced detection of Pine Wilt Disease: An image classification approach. Computers and Electronics in Agriculture, 218, 108690.

[4] Wang, D., Sun, Z., Huang, X., Liu, M., Zheng, Q., Zhang, H., & Zhang, G. (2024). Pine wood nematode disease area identification based on multi-temporal multi-source remote sensing images and BIT model. Geocarto International, 39(1), 2310117.

[5] Chen, Y., Yan, E., Jiang, J., Zhang, G., & Mo, D. (2023). An efficient approach to monitoring pine wilt disease severity based on random

sampling plots and UAV imagery. Ecological Indicators, 156, 111215.
[6] Lee, M. G., Cho, H. B., Youm, S. K., & Kim, S. W. (2023). Detection of pine wilt disease using time series UAV imagery and deep learning semantic segmentation. Forests, 14(8), 1576.
[7] Miao, J., Zhang, C., Yuan, M., & Gu, S. (2023, November). Detection of Pine Wood Nematode Infestation Based on Improved YOLOv5. In Journal of Physics: Conference Series (Vol. 2637, No. 1, p. 012029). IOP Publishing.
[8] Zhang, N., Chai, X., Li, N., Zhang, J., & Sun, T. (2023). Applicability of UAV-based optical imagery and classification algorithms for detecting pine wilt disease at different infection stages. GIScience & Remote Sensing, 60(1), 2170479.
[9] Xie, W., Wang, H., Liu, W., & Zang, H. (2024). Early-Stage Pine Wilt Disease Detection via Multi-Feature Fusion in UAV Imagery. Forests, 15(1), 171.
[10] Pan, J., Lin, J., & Xie, T. (2023). Exploring the potential of UAV-based hyperspectral imagery on pine wilt disease detection: Influence of spatio-temporal scales. Remote Sensing, 15(9), 2281.
[11] Thirumalraj, A., Chandrashekar, R., Gunapriya, B., & kavin Balasubramanian, P. (2024). Detection of Pepper Plant Leaf Disease Detection Using Tom and Jerry Algorithm With MSTNet. In Machine Learning Techniques and Industry Applications (pp. 143-168). IGI Global.
[12] Yu, R., Luo, Y., & Ren, L. (2024). Detection of pine wood nematode infestation using hyperspectral drone images. Ecological Indicators, 162, 112034.
[13] Tan, C., Lin, Q., Du, H., Chen, C., Hu, M., Chen, J., ... & Xu, Y. (2024). Detection of the Infection Stage of Pine Wilt Disease and Spread Distance Using Monthly UAV-Based Imagery and a Deep Learning Approach. Remote Sensing, 16(2), 364.
[14] Shen, J., Xu, Q., Gao, M., Ning, J., Jiang, X., & Gao, M. (2024). Aerial Image Segmentation of Nematode-Affected Pine Trees with U-Net Convolutional Neural Network. Applied Sciences, 14(12), 5087.
[15] Qin, B., Sun, F., Shen, W., Dong, B., Ma, S., Huo, X., & Lan, P. (2023). Deep learning-based pine nematode trees' identification using multispectral and visible UAV imagery. Drones, 7(3), 183.
[16] Yuan, Q., Zou, S., Wang, H., Luo, W., Zheng, X., Liu, L., & Meng, Z. (2024). A Lightweight Pine Wilt Disease Detection Method Based on Vision Transformer-Enhanced YOLO. Forests, 15(6), 1050.
[17] Xie, W., Wang, H., Liu, W., & Zang, H. (2024). Early-Stage Pine Wilt Disease Detection via Multi-Feature Fusion in UAV Imagery. Forests, 15(1), 171.
[18] Thapa, N., Khanal, R., Bhattarai, B., & Lee, J. (2024). Pine Wilt Disease Segmentation with Deep Metric Learning Species Classification for Early-Stage Disease and Potential False Positive Identification. Electronics, 13(10), 1951.
[19] Jung, Y., Byun, S., Kim, B., Amin, S. U., & Seo, S. (2024). Harnessing synthetic data for enhanced detection of Pine Wilt Disease: An image classification approach. Computers and Electronics in Agriculture, 218, 108690.
[20] Tan, C., Lin, Q., Du, H., Chen, C., Hu, M., Chen, J., ... & Xu, Y. (2024). Detection of the Infection Stage of Pine Wilt Disease and Spread Distance Using Monthly UAV-Based Imagery and a Deep Learning Approach. Remote Sensing, 16(2), 364.
[21] Gallo, I., Rehman, A. U., Dehkordi, R. H., Landro, N., La Grassa, R., & Boschetti, M. (2023). Deep object detection of crop weeds: Performance of YOLOv7 on a real case dataset from UAV images. Remote Sensing, 15(2), 539.
[22] Qin, J., Wang, B., Wu, Y., Lu, Q., & Zhu, H. (2021). Identifying pine wood nematode disease using UAV images and deep learning algorithms. Remote Sensing, 13(2), 162.
[23] He, Y.; Chen, G.; Potter, C.; Meentemeyer, R.K. Integrating multi-sensor remote sensing and species distribution modeling to map the spread of emerging forest disease and tree mortality. Remote. Sens. Environ. 2019, 231, 111238.
[24] A. Fan, E. Grave, and A. Joulin, ''Reducing transformer depth on demand with structured dropout,'' 2019, arXiv:1909.11556.
[25] J. Park, S. Woo, J.-Y. Lee, and I. S. Kweon, ''A simple and light-weight attention module for convolutional neural networks,'' Int. J. Comput. Vis., vol. 128, no. 4, pp. 783–798, Apr. 2020.
[26] Hayyolalam, V., & Kazem, A. A. P. (2020). Black widow optimization algorithm: a novel meta-heuristic approach for solving engineering optimization problems. Engineering Applications of Artificial Intelligence, 87, 103249.